Fault Localization In WDM Mesh Networks

Ehsan Sarvghad Moghaddam and Éva Hosszu

Supervisor:
János Tapolcai
Dept. of Telecommunications and Media Informatics
Faculty of Electrical Engineering and Informatics
Budapest University of Technology and Economics

Submitted:

October 28, 2011

Contents

Abstract

In recent years, according to deployment of DWM networks, fault detection and localization has become a major requirement in all optical networks due to providing network survivability and preventing huge data losschallenging issue in networks with high reliability. In upper layer monitoring schemes [1], although they need less hardware, complex signaling makes the fault localization a long process. In contrast, schemes at the optical layer can significantly reduce signaling [2, 3, 4]. In addition, they generally respond much faster to a failure event, therefore they are preferred in achieving fast link failure localization.

However, due to lack of optical/electrical/optical (O/E/O) regeneration in transparent optical networks, a single fault (e.g. fiber cut) can trigger a huge number of redundant alarms. This not only increases the management cost of the control plane but also makes failure localization difficult [5]. So, the fast and accurate fault localization is a major concern in all optical networks. We investigate optical layer monitoring schemes for fast link failure localization in WDM mesh networks related to the new concept monitoring trail (m-trail) which is proposed in [6]. It differs from the existing monitoring cycle (m-cycle) concept [7, 8] by removing the cycle constraint. As a result, m-trail provides a more flexible all-optical monitoring structure which includes simple, non-simple m-cycles and open trails as special cases.

On the other hand, Optical layer monitoring schemes based on monitoring trail (m-trail), is considered as the most efficient way to localize single fault unambiguously in all optical networks which is the most critical point in fault localization. Although the admirable works on m-trail concept, the issue has not been observed through feasibility point of view. However, previous works on m-trail monitoring scheme have focused on algorithm design for minimizing the number of monitors, whereas none of them has observed the limitations should be considered for length of it.

In this work, we investigate the physical constraints on launching m-trail focusing on the length of m-trails. We implemented VPI Transmission Maker Simulation Tool [9] to simulate different experiments for observing qualitative parameters in different m-trail length.

Chapter 1

Fault Detection And Localization

The problem of fault detection and localization has been widely studied in general communication networks as WDM (Wavelength Division Multiplexing) technology is widely deployed in the past decade. Due to the high-speed nature and the vulnerability of WDM-based all-optical networks, fast monitoring and fault localization schemes play a vital role in immediate traffic recovery against a particular component failure. A monitoring scheme monitors the health of the network and helps to localize a component failure, such as a fiber-cut which is the most common failure in optical networks. According to Bellcore statistics [10], the rate of fiber-cuts is about 1-5 cuts per 1000 km each year. If a fiber carries 160 wavelength channels and each operates at 10 Gbps (OC-192), a fiber-cut will result in 1.6 Tbps data loss. This leads to great economic damage, as our daily commercial, social and cultural activities have tremendously relied on Internet which is built on top of the optical backbone. If a link failure can be accurately localized in a timely manner, the disrupted traffic will be promptly rerouted to bypass the failed link. Accordingly, a fast monitoring scheme helps to minimize service downtime and data loss as well as economic damage.

Basically, either upper layer protocols or optical layer schemes can work alone for fault monitoring. In the case of optical layer schemes, the probe signals are sent onto a set of predetermined lightpaths for fault diagnosis purpose, where a lightpath is an all-optically connected path using a wavelength channel on each link along the path. Compared with optical layer monitoring schemes, upper layer protocols need less hardware support but more signaling efforts for fault monitoring. As a result, optical layer monitoring schemes generally respond much faster to a failure event, and thus is preferred in achieving fast link failure localization.

In an optical layer monitoring scheme, a link failure is detected and localized simply based on the on-off status of some supervisory optical signals [7, 8]. This requires additional wavelength channels to transmit the supervisory optical signals, and some special devices called monitors to check the on-off status and generate alarms upon a failure event, as shown in Figure 1. This hardware cost is necessary for achieving fast link failure localization at the optical layer, and is to be minimized as a major design objective. Meanwhile, reducing the required number of monitors has more significant importance, because it leads to less fault management efforts by managing only a small set of monitors. So, minimizing the number of required monitors (but without losing the accuracy of the failure localization) can greatly simplify fault management and make the network more scalable [5].

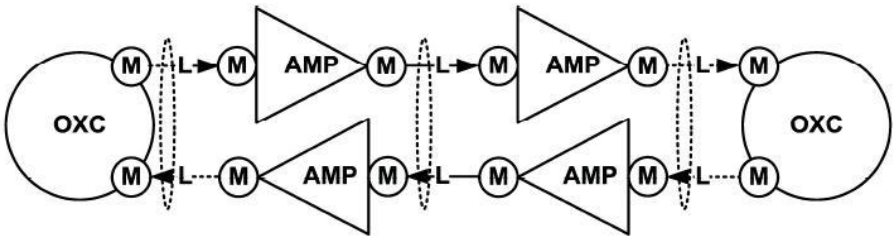

Figure 1.1: Monitor placement on a bi-directional fiber edge.

1.1 Fault Detection And Localization In WDM Meshed Networks

Most existing approaches related to fault detection and localization consist in deploying optical monitors responsible for generating alarms upon a single link failure. Monitoring in-formation (i.e. alarms generated by the monitors) are then submitted to the control plane of the optical network so that any routing entity is able to localize the failure and to perform a real time traffic restoration. In the proposed approaches, dedicated supervisory channels are used for monitoring purposes at the detriment of operational lightpaths. In other terms, supervisory channels cannot carry real traffic. Such monitoring schemes are referred to as "out-of-band monitoring" as opposed to "in-band monitoring" where monitors are supervising operational lightpaths [11].

In-band monitoring has been proposed in order to reduce the overhead induced by its counterpart out-of-band monitoring in terms of the number of dedicated lightpaths, required transponders and monitors, dedicated bandwidth, lightpath provisioning and maintenance, etc. In-band monitoring techniques are capable of monitoring individual wavelengths on each fiber and may also allow for estimation of the channel's performance. In this context, the objective is to optimally deploy optical monitors that will supervise already provisioned lightpaths in order to uniquely localize each network element failure. However, such an approach highly depends on the traffic itself and may need to evolve with time.

Hybrid approaches can be proposed as a mid-way solution between out-of-band and in-band monitoring schemes. In such approaches, the objective is to jointly use existing operational lightpaths in addition to a minimum set of complementary out-of-band lightpaths in order to achieve unambiguous failure localization.

The major concern of all previous approaches is to minimize the monitoring cost while achieving the unambiguous failure localization. For in-band monitoring schemes, monitoring cost is taken into account only for the numbers of required optical monitors. For hybrid and out-of-band monitoring schemes, the previous cost is augmented by the number of required laser diodes as well as the number of required supervisory channels [12].

Chapter 2

Main Paradigms For Out Of Band Monitoring

In this part we try to summarize out-of-band monitoring schemes for fault detection and localization in WDM networks. Based on different papers, we can clearly identify three main paradigms, namely conventional link-based monitoring (m-links), cycle-based monitoring (m-cycles) and trail-based monitoring (m-trails). So, first we try to review basic principle of each paradigm in the following.

2.1 Link Based Monitoring

In conventional link-based monitoring scheme, the position of the laser diodes/optical monitors is straightforward. Each fiber-link is equipped with a laser diode and an optical monitor at each of its ends, respectively. Moreover, an optical supervisory channel is reserved on each link in order to detect any failure occurring on that link. Consequently, this approach is able to detect and locate without any ambiguity any single link failure as well as multiple link failures in the network. Such a monitoring scheme costs $|E|$ laser diodes, $|E|$ optical monitors, and $|E|$ supervisory channels, where $|E|$ denotes the number of network links. For the network topology shown in Figure 2.1, a link-based monitoring solution requires 7 laser diodes, 7 monitors, and 7 supervisory channels. On the left-hand-side of Figure 2.1, we can see the monitoring information associated to each single link's failure.

	ℓ_a	ℓ_b	ℓ_c	ℓ_d	ℓ_e	ℓ_f	ℓ_f
a	1	0	0	0	0	0	0
b	0	1	0	0	0	0	0
c	0	0	1	0	0	0	0
d	0	0	0	1	0	0	0
e	0	0	0	0	1	0	0
f	0	0	0	0	0	1	0
g	0	0	0	0	0	0	1

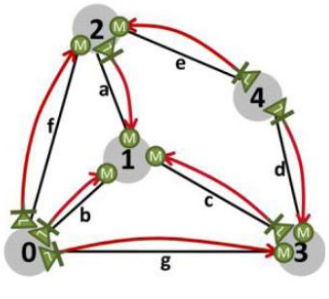

Figure 2.1: Link-based monitoring scheme.

To sum up, a link-based monitoring scheme requires one laser diode and one monitor per link and consumes one optical supervisory channel on each link of the network. Although this approach consumes the theoretical

minimum number of supervisory channels, it consumes an excessive number of laser diodes and optical monitors which makes it less attractive for large networks.

2.2 Monitoring Cycles

A network can be decomposed into a set of cycles so that all nodes and links in the network appear in at least one of these cycles as shown in Figure 2.2. An m-cycle is defined as a loopback connection associated with a laser diode-optical monitor pair [7, 8]. A supervisory optical signal is transmitted along the cycle consuming one optical channel on each link it traverses. If a failure occurs on a link, the supervisory optical signal will be disrupted and an alarm is generated by its associated monitor.

A monitoring scheme based on the concept of m-cycles generally consists of J m-cycles c_1,c_2,c_3,...,c_J that cover every link of the considered network. Upon a single link failure, monitors associated to the cycles traversing that link will generate alarms. Monitoring information produce an alarm code a_1,a_2,a_3,...,a_J, where a_i= 1 if cycle c_i traverses the failed link and 0 otherwise.

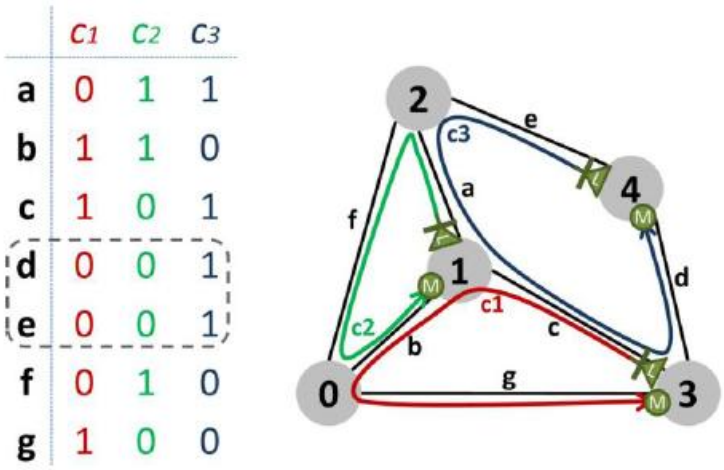

Figure 2.2: m-cycle based monitoring scheme.

From the table in Figure 2.2, we notice that 'link d' and 'link e' failures generate the same alarm code. Consequently, when receiving the alarm code [0,0,1], network operator is not able to precisely localize the failed link. One solution to eliminate such an ambiguity consists in using an additional link-based monitor either for 'link d' or 'link e' which increases the number of optical monitors as well as the number of required supervisory channels. However, the number of required monitors remains less than the 7 monitors required in a pure link-based monitoring scheme.

In summary, the m-cycles have been proposed with the objective to reduce the number of required laser diodes and optical monitors, and subsequently reducing the network monitoring cost. An m-cycle is a loop-back optical connection using a supervisory optical channel on each link it traverses, with a laser diode and an optical monitor placed back to back at any node along the loop. However, the major drawback of the m-cycles is their inability to distinguish in some cases between single link failures occurring on different links. These links usually belong to the same network segments; a segment is defined as a path made of at least two consecutive links where intermediate nodes have a nodal degree of two. In order to localize each link failure without any ambiguity, extra link- based monitors are required.

2.3 Monitoring Trail

As stated previously, an m-cycle monitoring scheme may not be able to distinguish between the failure of the different links of the same network segment. Consequently, a loopback monitoring scheme is not the best suited approach for network topologies containing segments.

In order to cope with ambiguity, the concept of monitoring trails (m-trails) has been introduced. M-trails break the structure of the cycle by assuming that the laser diode and the optical monitor are not necessarily collocated at the same node as shown in Figure 2.3. Although the cycle structure constraint is removed, an m-trail works exactly in the same way as an m-cycle for fast link failure localization. Moreover, an m-trail may be an m-cycle or a non-simple m-cycle (i.e. a non-simple m-cycle refers to an m-cycle that traverses the same node multiple times).

	t_1	t_2	t_3
a	0	1	0
b	1	0	0
c	1	1	0
d	1	0	1
e	0	0	1
f	0	1	1
g	1	1	1

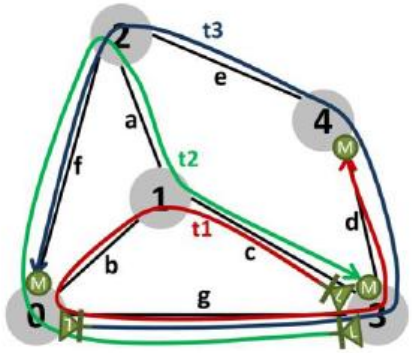

Figure 2.3: m-trails based monitoring scheme.

Similar to a non-simple m-cycle, an m-trail can traverse a node multiple times but it traverses a link at most once. From the table in Figure 2.3, we can see that an m-trail monitoring scheme is able to associate to each link in the network a unique alarm code and thus, to unambiguously locate any single link failure occurring in the network. In the considered example, the m-trails consume 3 laser diodes, 3 optical monitors, and 12 optical channels.

Concisely, the m-trails have been proposed as an alternative for the m-cycles with the objective to localize without any ambiguity any single link failure while still reducing the number of required laser diodes and optical monitors. An m-trail works in the same way as an m-cycle, but the optical connection of the supervisory channels does not necessarily need to be a loop. Thus, the laser diode and the optical monitor are not necessarily collocated together to maintain the cycle structure. As a result, both link-based and m-cycles monitoring are special cases of m-trails. As the result, the m-trail approach tries to find a tradeoff between the cost penalty due to the additional number of supervisory channels and the cost benefit due to the reduction of the number of laser diodes and optical monitors.

If we construct a model based on an enumeration-free Integer Linear Program (ILP) approach, m-trail is proved to yield much better performance by employing monitoring resources in the shape of trails - a monitoring structure that generalizes all the previously counterparts. However, due to the huge computation complexity in solving the ILP, only network topologies with small sizes (such as 30 nodes) can be handled.

Chapter 3

The M-Trail Design Problem

Without loss of generality, the target of m-trail design is to minimize the cost function determined by the weighted sum of management cost and bandwidth cost [5]. The management cost generally accounts for the fault management complexity in terms of the length of alarm code, which further affects the number of alarms flooded in the network when a failure event occurs. In addition to larger fault management cost, a longer alarm code may cause a longer failure recovery time since a network entity has to collect all the necessary alarm signals for making a correct failure localization decision. The bandwidth cost reflects the additional bandwidth consumption for monitoring, which is measured by way of the cover length of an m-trail solution (i.e., the sum of lengths of m-trails in the solution). Here, the length of an m-trail is taken as the number of links traversed by the m-trail. The target function adopted in the study is:

$$\begin{aligned} \textit{Total Cost} &= \textit{management cost} + \textit{bandwidth cost} \\ &= \gamma \times (\textit{no. of m-trails}) + \textit{cover length} \end{aligned} \tag{3.1}$$

where the cost ratio γ determines the relative importance of management cost and bandwidth cost, which should be defined according to the carrier operational target.

In order to achieve Unambiguous Failure Localization (UFL), each link must be assigned with a unique binary alarm code [a_1, a_2,..., a_J], where J is the length of alarm code, and a_j is binary digit, which is 1 if the j^{th} m-trail traverses through this link and 0 otherwise. The m-trail t_j has to traverse through all the links with a_j = 1 while avoiding to take any link with a_j = 0. Let L_j denote the j^{th} link set which contains the set of links with a_j = 1. The link set L_j forms an m-trail t_j if there is a non-simple path that traverses through all the links in L_j but no any other. This is referred to as m-trail formation. Here, the theoretical lower bound on J is $\lceil \log_2 (|E| + 1) \rceil$, since there are $|E|$ single failure states plus the no failure state. However, due to the network topology limitation and possibly other design objectives (e.g., the bandwidth consumption limitation), an m-trail solution could take more than $\lceil \log_2 (|E| + 1) \rceil$ m-trails [5].

3.1 Algorithm for M-Trail Solution

A novel algorithm for achieving a fast and efficient m-trail design in general topologies is introduced in this section [5]. The proposed algorithm takes advantage of random code assignment (RCA) and random code swapping (RCS), aiming to overcome the topology diversity that has became problematic for ILP formulation of m-trail. With RCA, it takes $|E|$ unique alarm codes which are randomly assigned to each link one after the other at the beginning and is kept in an alarm code table (ACT). This leads to $\lceil \log_2 (|E| + 1) \rceil$ link sets. The algorithm then performs m-trail formation by examining the connectivity of each link set. There could be much more m-trails than $\lceil \log_2 (|E| + 1) \rceil$

formed at the beginning. To improve the solution quality, RCS is performed to update the ACT for each link set round by round, where a better structure of a link set is searched according to the cost function. In the design, RCS is performed independently (or locally) at each link set, where the codes of two links of different link sets can be swapped only if the swapping will not alter the connectivity of the other link sets. This is referred to as the strong locality constraint (SLC), which is an important feature of the design in making the algorithm simpler and running faster.

3.1.1 Random Code Swapping (RCS)

The initial RCA may yield an unqualified result that contains many isolated fragments and a large number of odd-degree nodes. This subsection describes the proposed RCS mechanism for shaping the links of a link set into one or a number of m-trails while still meeting the overall Unambiguous Failure Localization (UFL) requirement. The key idea of the proposed RCS mechanism is the strong locality constraint (SLC) which governs the swapping mechanism in each link set. It means that the alarm code of a specific link in L_j can be swapped with that of a link not in L_j if all the other link sets are not affected due to the swapping. The necessary condition for meeting the SLC is that the alarm codes of two links in L_j are bitwise identical except for a single bit at position j. Such a code pair is called a code pair of L_j, and the two links corresponding to the code pair form a bitwise link-pair of L_j. For example, 1011011 and 1010011 form a code pair of L4, and the corresponding links form a bitwise link-pair of L_4. Thus, swapping alarm codes of the two links meets the SLC due to the local influence on L_4. With the SLC, the RCS on a link set can be performed independently from the others. This mechanism allows easy implementation and provides high efficiency.

Note that for L_j, some links may not have a bitwise link-pair due to two reasons:

1. its code pair of L_j is all 0's, which does not correspond to any failure state. For example, 010000 is a code pair of 000000 of L_2, but there is not a link corresponding to the alarm code 000000.

2. The code pair of L_j of the link was not assigned to any link. In this case, the unassigned code can be freely used by the link without violating the SLC.

In summary, RCS is performed on each link set by randomly swapping alarm codes of all bitwise link-pairs of the link set, in order to help interconnecting isolated trail fragments and reducing the number of odd-degree nodes in the link set iteratively in each greedy cycle.

3.1.2 An Example of RCS Algorithm

An example is provided as follows to show how RCS is performed [5]. The 26-node US network with 42 links are uniquely and randomly coded in 6 bits at the beginning. Figure 3.1 shows the link set assigned to the lowest bit (i.e., the 6^{th}). Except for the link between Denver and Kansas City that was assigned with an alarm code 0000001, all the other links either have a bitwise link-pair in L_6 , or are don't-care links of L_6. Figure 3.2 shows each link-pair at L_6 by an arrow. For example, (Atlanta, Charlotte) link and (Indianapolis, Cleveland) link are bitwise link-pairs of L_6. It can be easily seen that swapping the two links will interconnect two isolated fragments and reduce the number of odd-degree nodes by two, which leads to a saving of an m-trail. Similarly, swapping link (Salt Lake City, Denver) with link (Houston, New Orleans) will not increase the total cost of the ACT. While in the subsequent greedy cycle, swapping link (Las Vegas, El Paso) with link (El Paso, Houston) would further reduce the number of m-trails through the RCS and thus possibly reduce the total cost. With more greedy steps on those link pairs and don't-care links of L_6, it is possible to form a single m-trail corresponding to the 6th bit in the Alarm Code Table (ACT) while keeping all other link sets not modified. By iterating the greedy process for each bit in the ACT, the algorithm can guarantee to obtain an m-trail solution for each bit in the ACT.

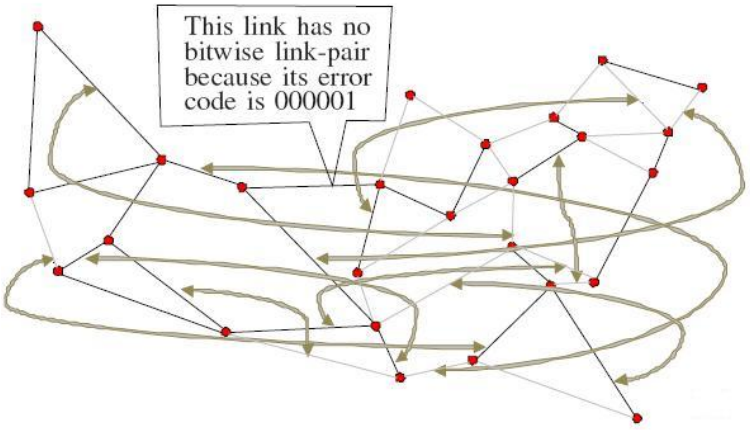

Figure 3.1: random code swapping.

Figure 3.2: after greedy random code swapping.

3.1.3 Constrained Trail Reconfiguration

In this section we describe an algorithm which improves the quality of an m-trail solution by reconfiguring certain m-trails [13]. The algorithm takes a trail to reshape, the set of links to add and the set of links to avoid as an input. First it assigns a null weight to all the links which must be included in the final solution and an infinite weight to all the links which must be removed from the trail. All the remaining links in the network are assigned a weight equal to 1. These links are referred to as *undesirable links*. The CTR algorithm aims at constructing a valid trail that contains all the links with a null weight while avoiding the undesirable links as much as possible.

The algorithm carries this out by using a Best-First Search approach. The basic solution is constructed by choosing a link with null weight and putting it in a queue list. The algorithm then takes a solution from the list and attempts to construct a new m-trail solution by adding additional links at either end of the trail and avoiding all the trails with infinite cost at the same time. The following flowchart depicts the algorithm in detail.

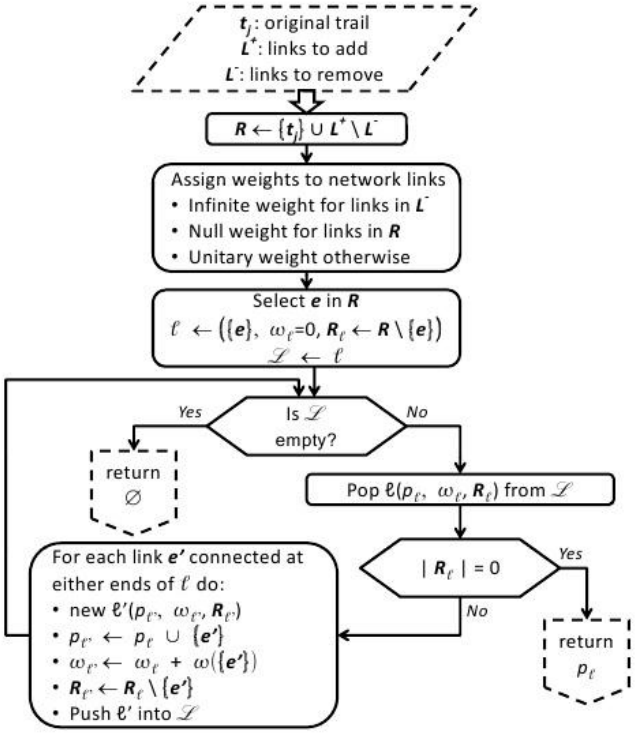

Figure 3.3: Flowchart of the CTR algorithm.

In our simulations we use CTR initialized with an m-trail solution from RCS. Now let's see an example on how the CTR algorithm works. Consider the following m-trail solution.

We focus on trail t_1 and try to reconfigure it by adding link d and removing link a. In order to do this the algorithm first assigns infinite weight to link a, null weight to links b, c, g and d and weight 1 to links e and f. After that the algorithm starts building a new trail by considering a link with null weight, let this be link g (see Figure 3.4). To this first solution we can add at either end of the trail one of the following links: b, c, d or f. For each possibility we define a new solution and update its weight by the addition of a new link, see Figure 3.4. Next we select one of the unprocessed trails with the lowest weight, let this be the uppermost one on the figure. To this solution we can add link a, c or d at either end of the trail (note that link c can be added either by connecting it to node 1 or node 3). Now we repeat the step defining a new solution for each possibility and updating its weight by the addition of a new link. In this example this gives for new solutions. If we add link a it results in infinite weight, we ignore that. The previous unprocessed trails are still in the set of possible trails (see the figure). This set gives 6 possible trail solutions, so we select the one with the lowest weight. Repeating this steps makes the CRT algorithm tend to a single trail, in this example it is the trail consisting of links d, c, b and g. Note that the solution does not contain any undesirable links.

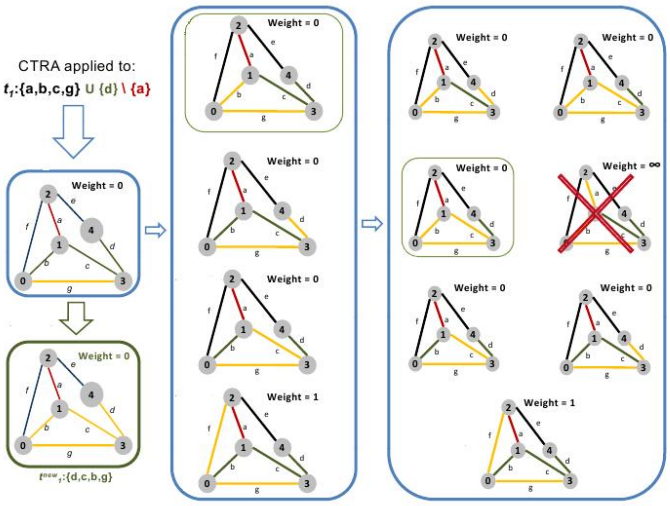

Figure 3.4: CTR algorithm applied to trail t_1 with the aim of adding link d and removing link a.

3.1.4 Integer Linear Programming

Using ILP formulation, we can generate an optimal m-trail solution to minimize the monitoring cost defined in (3.1) while achieving unambiguous failure localization. Given a network topology $G(V, E)$, the cost c_{uv} of a supervisory wavelength for each link $(u, v) \in E$ and the cost ratio γ of a monitor to a supervisory wavelength-link, the following equations formulate the problem [14].

Objective:

$$\gamma \sum_{j} m^j + \sum_{j} \sum_{u,v \in E} c_{uv}(e^j_{uv} + e^j_{vu}) \rightarrow \min; \tag{3.2}$$

Subject to:

$$\sum_{u \in V} t^j_u \leq 1, \forall j; \tag{3.3}$$

$$\sum_{u \in V} r^j_u \leq 1, \forall j; \tag{3.4}$$

$$\sum_{u \in V} (e^j_{uv} - ej_{vu}) = t^j_u - r^j_u, \forall u \in V, \forall j; \tag{3.5}$$

$$e^j_{uv} - e^j_{vu} \leq 1, \forall (u, v) \in E, \forall j; \tag{3.6}$$

$$z^j_u \geq e^j_{uv} - e^j_{vu}, \forall u \in V : (u, v) \in E, \forall j; \tag{3.7}$$

The list of notations used in the equations:

- J : The maximum number of m-trails allowed in the solution.
- j : m-trail index, where $j = 0, 1, \ldots, J-1$.
- E : The set of all the links in the topology.
- V : The set of all the nodes in the topology.
- c_{uv} : Predefined cost of a supervisory wavelength on link (u,v), whose default value is 1.
- L : Predefined length-limit on each m-trail.
- γ : Cost ratio defined in section 3.
- e^j_{uv} : Binary variable with value 1, if $u \rightarrow v$ is an on-trail vector of the m-trail t_j, 0 otherwise.
- t^j_u : Binary variable with value 1, if u is the transmitter on m-trail t_j, 0 otherwise.
- r^j_u : Binary variable with value 1, if u is the receiver on m-trail t_j, 0 otherwise.
- z^j_u : Binary variable with value 1, if node u is traversed by m-trail t_j, 0 otherwise.

The objective aims at minimizing the monitoring cost described in (3.1). Constraints (3.3) and (3.4) ensure that there is only one transmitter and receiver node in each m-trail t_j. Constraint (3.5) formulates the flow conservation property at each node, that is, if a node u is neither T nor R, it must have an equal number of inbound and outbound vectors. If $u = T$ then $t_u^j - r_u^j = 1$ and if $u = R$ then $t_u^j - r_u^j = -1$. Finally constraint (3.7) allows at most a single directed vector on each link (u,v), either $u \to v$ or $v \to u$ or none.
If we want to place a length limit on each m-trail, we can do so by adding the following constraint to the ILP problem.

$$\sum_{(u,v)\in E} c_{uv}(e_{uv}^j + e_{vu}^j) \leq L \tag{3.8}$$

The ILP formulated above gives a valid m-trail solution.

3.2 Simulation Results

3.2.1 Placing a length limitation

Since there are physical limitations as to how long m-trails are realizable, it is interesting to examine what happens when the length of m-trails are limited. We used ILOG CPLEX 11.0 [15] to implement the ILP on a server with 3GHz Intel Xeon CPU 5160. Figure 3.2.1 and Table 3.5 show two examined topologies and its details, the Deutsche Telekom described in Section 5.2 and a larger Pan-European network.

Parameters	**Pan-European**	**Deutsche Telekom**
Number of nodes	16	17
Number of links (bidirectional)	23	26
Network diameter	6	7
Minimal nodal degree	2	2
Maximal nodal degree	4	6
Average nodal degree	2,88	3,06
Physical connectivity	0,19	0,19
Shortest link	218 km	36 km
Longest link	783 km	353 km

Figure 3.5: Parameters of the Pan-European and the Deutsche Telekom network

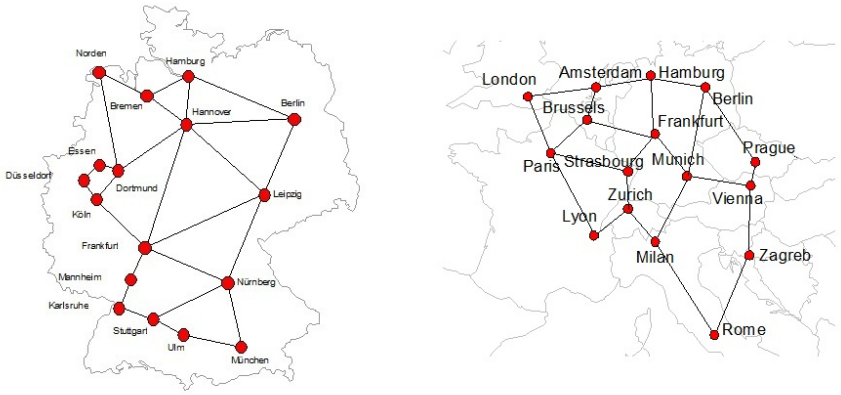

Figure 3.6: The Deutsche Telekom and the Pan European network

The following figure shows the results from the ILP algorithm with different length limits on m-trails. It can be observed that m-trails are relatively long in small networks compared to the total size of the network. For example in Deutsche Telekom network to achieve unambiguous failure localization with the minimum number of m-trails, some m-trails reach more than 6000^{km}, which is long compared to the size of networks. The reason is that for efficient failure localization, each m-trail should test the status of approximately the half of the links in the network. Note that total cable length in Deutsche Telekom network is 10750^{km}, thus the half it (5375) gives a good approximation on the approximate length of the m-trail solution with minimum number of m-trails. However, limiting the length of each m-trail by 50% requires 1.7 times more m-trails to achieve unambiguous failure localization. In the larger Pan-European network to achieve unambiguous failure localization with the minimum number of m-trails, the m-trails are 50% longer than for Deutsche Telekom Network.

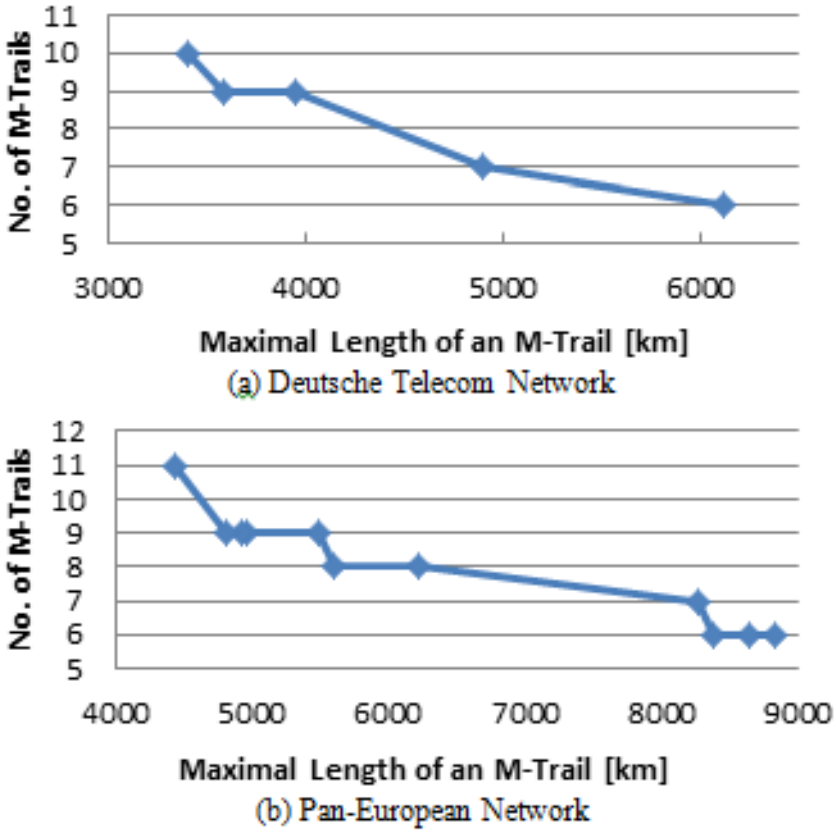

Figure 3.7: Parameters of the Deutsche Telekom and the Pan-European network

Unfortunately, the runtime of the ILP for larger networks was unacceptable. To achieve unambiguous failure localization with minimum number of m-trails on the 26-node US network with 42 links requires m-trails with length of 10306km [5], which is still smaller than the maximum length limit of 15000 km. However it was 18037 km for the 37-node European fiber-optic network defined by IST project LION and COST action 266 as [16], which has 57 bi-directional links.

3.2.2 Lower bound on the number of m-trails

In this subsection we examine the performance of the m-trail forming algorithms described above as in how many m-trails an algorithm uses to find a valid m-trail solution as opposed to how many are necessary. We do this by applying a lower bound of Katona [17] on separating systems over a set H_n of n elements.

We call a system $\mathcal{A} = A_1, \ldots, A_m$ of subsets of a set H a separating system, if for any two distinct elements in H there exists a set in $\mathcal{A}$ containing exactly one of them. In other words, $\mathcal{A} = A_1, \ldots, A_m$ is a separating system, if for any two distinct elements x and y in H there exists A_i in $\mathcal{A}, i \in \{1, 2, \ldots, m\}$ such that either

$$x \in A_i, y \notin A_i,$$

or

$$x \notin A_i, y \in A_i.$$

This is exactly what unambiguous failure localization and a valid m-trail solution mean. If we also want to place a length limitation on m-trails, that is, if in addition it is required that each subset in the separating system should

consist of at most k elements, a lower bound was given on the number of subsets in the separating system by Katona.

Theorem 1. *Let S_K denote separating systems where each subset consists of exactly k elements. If $\{A_1, A_2, \ldots, A_m\} \in S_K$, then*

$$\frac{\log n}{\frac{k}{n}\log\frac{n}{k} + \frac{n-k}{n}\log\frac{n}{n-k}} \leq m,$$

where $\log$ *denotes logarithm with base* 2*. Using the inequality* $\ln(1+x) < x$ *we can obtain a weaker, but simpler estimation*

$$\frac{n\log n}{k\log\frac{en}{k}} \leq m.$$

Proof of the weaker estimation [18]. Let us consider the following. Suppose somebody chooses an element $x \in H$ and we seek for it by asking a sequence of questions: $x \in A_1$?,..., $x \in A_m$? where $A_i \subset H, i = 1, \ldots, m$. This strategy is successful if the answers are always sufficient to identify x. Obviously this is equivalent to $A_1, \ldots, A_m$ being a separating system. Let $A_1, \ldots, A_m$ where $m = m(n,k)$ be a minimal separating system and let p be the uniform distribution on H. Let x be the element we are searching for, now chosen randomly. Let Y_i denote the indicator of $x \in A_i$ and $H^*(q)$ the entropy function, that is,

$$H^*(q) = -q\log q - (1-q)\log 1 - q$$

.

Since H^* is increasing for $q \in [0, \frac{1}{2}]$ and $k < \lfloor \frac{n}{2} \rfloor$, for the entropy of Y_i we can write

$$H(Y_i) = H^*(A_i/n) \leq H^*(k/n).$$

On the other hand the vector $(Y_1, \ldots, Y_m)$ takes n distinct values because $A_1, \ldots, A_m$ is a separating system, therefore $H(Y_1, \ldots, Y_m) = \log n$. Because of the properties of the entropy function

$$H(Y_1, \ldots, Y_m) \leq \sum_{i=1}^{m} H(Y_i).$$

We can conclude that

$$\log n \leq m(n,k)H^*(k/n).$$

From here the lower bound follows by easy calculation.

□

The previous theorem is for the case when every subset consists of exactly k subsets as opposed to at most k elements, when applying it to m-trails. It is easy to see that it is sufficient to consider the exactly k elements-case, which means we can apply this estimation directly.

We have compared the performance of the ILP formulation and the CTR algorithm initialized with RCA-RCS with this lower bound on numerous topologies. The following table indicates the number of links and nodes in the topology, the maximal length of m-trails and the number of m-trails used in the solution by the algorithms. Obviously when dealing with the lower bound, one can use the ceiling integer of it.

links	nodes	maximal trail-length	lower bound	m-trails with ILP	m-trails with CTR
9	6	4	4	5	6
10	7	5	4	9	4
15	12	7	4	5	14
26	17	11	5	5	20
33	19	10	6	9	29
36	20	13	6	7	31
37	17	16	6	6	25
38	22	11	7	9	32
43	26	13	7	9	39
76	36	14	10	too big	67

As the table shows, the ILP algorithm performs quite well, with the m-trail solution being what the lower bound predicts or a little bit more than that. On the other hand, the CTR algorithm yields relatively bad solutions. On the plus side, its runtime is much quicker, and it can handle certain cases the ILP algorithm couldn't, namely when the network is too big or when there are approximately the same number of nodes and links (with more links of course).

Now let's see a detailed performance of the ILP-algorithm on a 36-link network. The table describes the results the ILP algorithm gave. On the figure below the curve indicates the lower bound for $n = 36, 10 \geq k \geq 16$ and the step function indicates the ceiling integer of the lower bound. The points indicate the number of m-trails the algorithm constructed a solution with.

maximal trail length	number of m-trails	lower bound
16	6	6
15	7	6
14	7	6
13	7	6
12	8	6
11	8	6
10	8	7

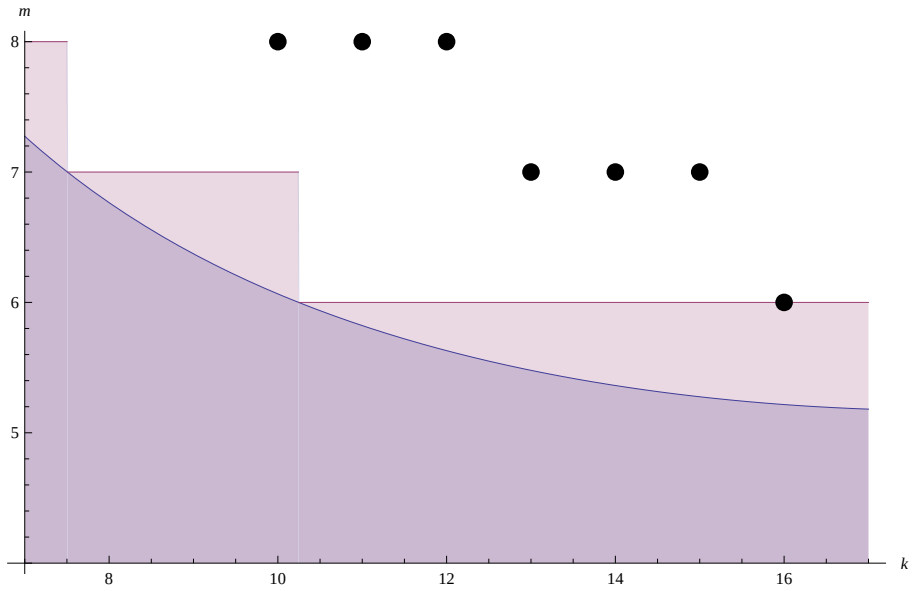

Figure 3.8: Number of m-trails with ILP compared to the lower bound

As these figures show, the ILP algorithm performs quite well, with the m-trail solution being what the lower bound predicts or a few trails more than that.

Chapter 4

Physical Layer Impairments

As optical signals traverse the optical fiber links, it is affected by transmission impairments induced by non-ideal components. Physical layer impairments can be classified into linear and nonlinear effects. Linear impairments are independent of the signal power and affect each of the wavelengths (optical channels) individually, whereas nonlinear impairments affect not only each optical channel individually but they also cause disturbance and interference between them [19].

4.1 Linear Impairments

The important linear impairments are:Fiber Attenuation, Amplified Spontaneous Emission (ASE) Noise, Chromatic Dispersion (CD) (or Group Velocity Dispersion (GVD)), Polarization Mode Dispersion (PMD).

4.1.1 Amplified Spontenous Emission (ASE) Noise

Amplifiers are placed periodically at each span to boost signal power. Each amplifier stage adds own component of ASE noise and degrades the OSNR [20]. The amplifier noise is quantified by noise figure (NF) value, which is the ratio of the optical signal to noise ratio (OSNR) before the amplification to the same ratio after the amplification and is expressed in dB [21].

Given the amount of gain G and the spontaneous emission factor nsp, the power spectral density of noise introduced by the amplifier is [22]:

$$G_{ASE}(f) = 2 \times n_{sp} \times (G - 1) \times h \times f \tag{4.1}$$

where h is the Planck constant and f is the operation frequency.

4.1.2 Chromatic Dispersion (CD)

Chromatic dispersion is a broadening of the input signal as it travels in the optical fibers. It affects the receiver performance by reducing the pulse energy within the bit slot and spreading the pulse energy beyond the allocated bit slot leading to inter-symbol interference (ISI) [19]. It contains both material dispersion and waveguide dispersion. Both of these phenomena occur because all optical signals have a finite spectral width, and different spectral components will propagate at different speeds along the length of the fiber. CD can be adequately (but not optimally) compensated for a per-link basis.

4.1.3 Polarization Mode Dispersion (PMD)

Polarization Mode Dispersion (PMD) is a broadening of the input pulse due to a phase delay between input polarization states. In optical fibers, mechanical and thermal stresses introduced during manufacturing, cause asymmetries in the fiber core geometry. It introduces small index of refraction differences for the two polarization states, a property called birefringence. Birefringence causes one polarization mode to travel faster than the other. PMD is negligible up to the 10 Gbps, however it becomes a critical factor for 40 Gbps or higher rates. In general, in combination with PMD there is also Polarization Dependent Loss (PDL). It can cause optical power variation, waveform distortion and signal-to-noise ratio fading [19].

4.2 Non-Linear Impairments

In reality, all materials behave nonlinearity at high intensities and their refractive index increases with intensity with respect to the following formula:

$$n = n_1 + n_2 \times (\frac{P}{A_{eff}}) \tag{4.2}$$

where n_2 is the nonlinear-index coefficient, P is the optical power, and Aeff is the effective mode area. The numerical value of n_2 is about $2.6 \cdot 10^{-20} \frac{m^2}{W}$ for silica fibers. Although the nonlinear part of the refractive index is quite small ($< 10^{-12}$ at the power level of 1^{mW}), it influences considerably networks of long fiber lengths. In particular, it leads to the phenomena of Self Phase Modulation (SPM), Cross Phase Modulation (XPM) [23].

4.2.1 Self Phase Modulation (SPM)

By using equation (4.2), it can be found that the propagation constant becomes power dependent. It can be written as:

$$\beta' = \beta + k_0 \times n_2 \times (\frac{P}{A_{eff}}) = \beta + \gamma \times P \tag{4.3}$$

where $\gamma = 2 \times \pi \times (\frac{n_2}{A_{eff}\lambda})$ is an important nonlinear parameter with value ranging from 1 to 5 $\frac{w^{-1}}{km}$ depending on the value of Aeff and the wavelength. Consequently, optical phase increases linearly and the term produces a nonlinear phase shift given by

$$\psi_{NL} = \int_0^L (\beta' - \beta)\, dz = \int_0^L \gamma P(z)\, dz = \gamma P_{in} L_{eff} \tag{4.4}$$

In practice, time dependence of Pin makes ψ_{NL} to vary with time. In fact, the optical phase changes with time in exactly the same fashion as the optical signal. Since this nonlinear phase modulation is self induced, the nonlinear phenomenon responsible for it is called Self Phase Modulation (SPM). This SPM leads to frequency chirping of optical signal which is proportional to $\frac{dP_{in}}{dt}$ and depends on the pulse shape. It affects the signal by pulse broadening which increases the signal bandwidth considerably and limits the performance of the system [23].

4.2.2 Cross Phase Modulation (XPM)

The intensity dependence of the refractive index in equation (4.2) can also lead to another phenomenon known as Cross Phase Modulation (XPM). It occurs when two or more optical channels are transmitted simultaneously inside an optical fiber using the WDM technique. In such systems, the nonlinear phase shift for a specific channel depends not only on the power the channel but also on the power of other channels [23].

4.2.3 Four Wave Mixing (FWM)

The power dependence of the refractive index seen in equation (4.2) has its origin in the third-order nonlinear susceptibility denoted by $\chi(3)$. The nonlinear phenomenon, known as four-wave mixing (FWM), also originates from $\chi(3)$. If three optical fields with carrier frequencies ω_1, ω_2, and ω_3 co-propagate inside the fiber simultaneously, $\chi(3)$ generates a fourth field whose frequency ω_4 is related to other frequencies by a relation $\omega_4 = \omega_1 \pm \omega_2 \pm \omega_3$. Several frequencies corresponding to different plus and minus sign combinations are possible in principle. In practice, most of these combinations do not build up because of a phase-matching requirement. Frequency combinations of the form $\omega_4 = \omega_1 + \omega_2 - \omega_3$ are often troublesome for multichannel communication systems since they can become nearly phase-matched when channel wavelengths lie close to the zero-dispersion wavelength. In fact, the degenerate FWM process for which $\omega_1 = \omega_2$ is often the dominant process and impacts the system performance most [23].

4.3 Impairment Monitoring

As all-optical networks have been considered as the most reliable and economic solution to achieve high transmission capacities with relative low cost, signal quality has become a critical parameter in transmission of optical signals. In these networks, the signal remains in the optical domain. So, it brings a big challenge to manage these networks: providing quality of service (QOS). Therefore, we need efficient tools to monitor several physical impairments.

4.3.1 Optical Signal To Noise Ratio (OSNR)

Optical signal to noise ratio (OSNR) is an important figure of merit used in fiber link planning. It is the ratio of signal power to noise power, over a specific spectral bandwidth, at any point in an optical link. Noise power can be defined as any undesirable signal interference. All fiber transmission signals consist of modulated light with some level of background noise. As the noise level increases, the receiver has greater difficulty decoding signal information and consequently errors are introduced into the received transmission. A well-designed system will have sufficiently high receiver signal power over noise power (the OSNR) to maintain communications within acceptable error limits. All optical receivers can tolerate a minimum level of noise power below the signal power. This noise power is referenced to the signal power and is specified for the receiver as the minimum required OSNR value for a specific receiver signal power. If it is exceeded, transmission bit errors above the specification level will occur.

Noise sources can be grouped as active and passive. Active sources such as lasers, receivers, and optical amplifiers generate new noise power in the fiber link. Passive sources such as fiber, connectors, splices, and WDMs cause interference by distorting or reflecting the propagating signal power.

For most fiber transmission systems, OSNR needs to be considered only if optical amplifiers are included in a transmission link. This is because in links without amplifiers, noise power does not accumulate sufficiently to be a significant limiting factor.

OSNR can be defined as the logarithmic ratio of average optical signal power to average optical noise power over a specific spectral bandwidth measured at the input of an optical receiver photodiode.

$$OSNR = 10 \log \left(\frac{P_{signal}}{P_{noise}} \right) \tag{4.5}$$

Where P_{signal} is the signal power and P_{noise} is the noise power.

4.3.2 Bit Error Ratio (BER)

Bit error ratio (BER) can be defined as the ratio of the number of erroneous bits received to the total number of bits transmitted. It is defined in equation (4.5):

$$BER = \frac{E}{N} \tag{4.6}$$

$$N = T \times R \tag{4.7}$$

Where E is number of erroneous bits received, n is number of bits transmitted, T is the time to transmit n bits (second) and R is transmission rate (bits/second).

Ideally the BER test is run for an infinite amount of time, transmitting an infinite amount of bits, which results in the channel's true bit error ratio. However this is obviously not practical and therefore a statistical method is used to determine the channel's BER within a certain confidence level. This confidence level is a percentage that represents the probability the true BER is equal to or better than the test BER. Typical confidence levels are 95% or 99%. Calculation of the required number of transmitted bits for a certain confidence level is based on the binomial distribution model.

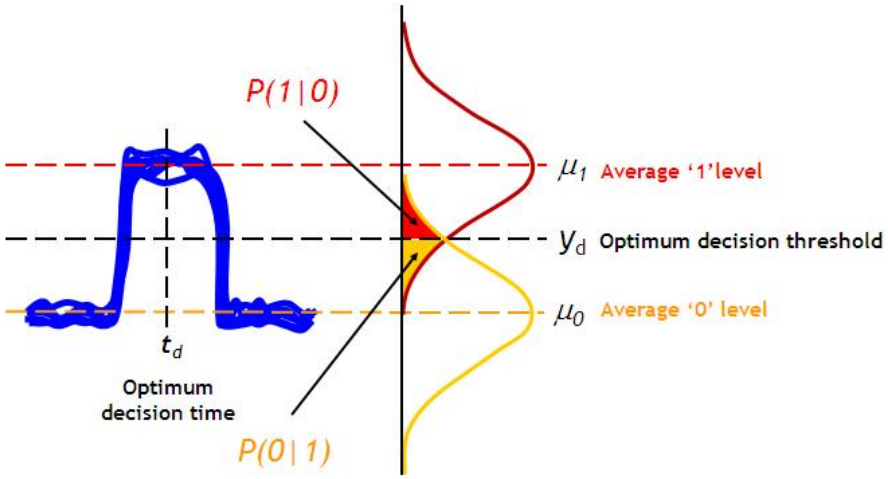

Figure 4.1: Bit Error Ratio calculation.

If we consider two level modulation, due to noise, the '1' level and the '0' level are not fixed. It not only varies from bit to bit, but also fluctuates within a bit. Over many number of bits, the '1' and '0' levels are statistically represented by distributions, each with its own mean and variance. Also, the noise power in the '0' and '1' levels is given by the respective variance. So, we can calculate BER as:

$$BER = p(1)p(0|1) + p(0)p(1|0) \tag{4.8}$$

Where $p(1)$ is the probability of '1' transmitted, $P(0)$ is the probability of '0' transmitted, $p(0|1)$ is the probability of detecting a '0' given that a '1' is actually received and $p(1|0)$ is the probability of detecting a '1' given that a '0' is actually received. It is shown in Figure 4.1.

4.3.3 Q Factor

The Q Factor is another performance parameter that can be used as an alternative to BER testing and can be used for performance planning during system design stage. Designing a system for a specific Q Factor that considers link impairments and gains such as Forward Error Correction (FEC) is straightforward and has good accuracy. Q

Factor is defined as the ratio of the difference of average photodiode currents between one bit state and zero bit state divided by the sum of the standard deviation (RMS) of the noise currents for both states.
If we consider two level modulations, Q is defined for any signal for which the mean levels μ_1 and μ_0, and the noise powers δ_1^2 and δ_0^2 can be sensibly defined, even if the noise is not Gaussian. The calculation for Q-factor is shown in Figure 4.2.
Moreover, the Bit Error Ratio can be calculates based on Q Factor: $BER = \frac{1}{2} erfc(\frac{Q}{\sqrt{2}})$.

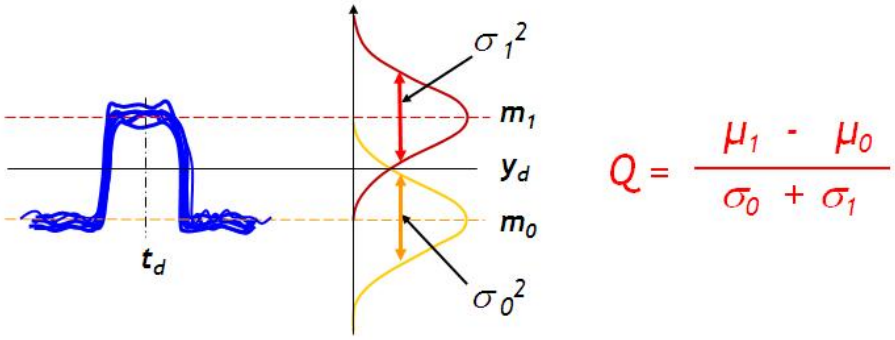

Figure 4.2: Q Factor calculation.

Chapter 5

Deployment Of M-Trail

5.1 Network Configuration

Figure 5.1 shows the typical configuration of a WDM transmission system. Transponders are used to adapt the signal for transmission. After adaptation, the wavelengths are multiplexed to form a composite signal. Nowadays, Single Mode Fiber (SMF) is implemented widely due to low attenuation. Before sending the signal to the fiber line, pre-amplification is necessary. Moreover, it becomes critical in DWM systems with a lot of spans due to increasing non-linearity. To compensate the fiber losses and dispersion, amplifiers should be used at each span. Each amplifier is composed of two Erbium-doped Fiber amplifiers (EDFAs) separated by a section of Compensating Dispersion Fiber (DCF). At the receiver side, the signal is post-amplified and de-multiplexed in order to recover the individual signals. Transponders at the receiver side correspond to photo-detectors. In the following, we call an m-trail the set of fiber spans connecting the source node to monitor.

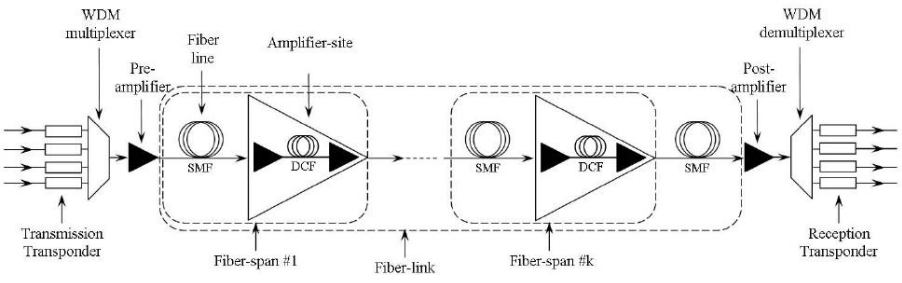

Figure 5.1: Typical configuration of WDM Transmission System.

The fiber lines are inter-connected through Optical Cross Connects (OXCs) which do not proceed to 3R electrical regeneration.
We have done our simulations based on European Backbone Network (EBN) parameters. Table 5.1 summarizes transmission parameters adopted in our simulations. We assumed each fiber span 60^{km} (it is become optimal through simulation). For simplification, we only consider one channel. However, due to setting the amplifiers output to appropriate low power (1^{mW}), the other channels effects (crosstalk, FWM and XPM) can be considered negligible. We consider the Q factor as a good parameter to characterize the transmission performance of optical path. It is an efficient way to characterize the signal quality at the Monitor. The admissible Q factor is considered equal to 4 that it corresponds to a BER of 10^{-5}. Besides, Figure 5.1 shows the network simulation in VPI.

Table 5.1: Transmission System Parameters

Parameter	Value
SMF losses (dB/km)	0.2.
SMF Dispersion (ps/nm.km)	17.
SMF PMD (ps/$\sqrt{(km)}$)	0.1.
DCF losses (dB/km)	0.6.
DCF Dispersion (ps/nm.km)	-90.
DCF PMD (ps/$\sqrt{(km)}$)	0.1.
Amplifier Type	EDFA Flat.
EDFA Noise Figure (dB)	4.
Q factor threshold	4.

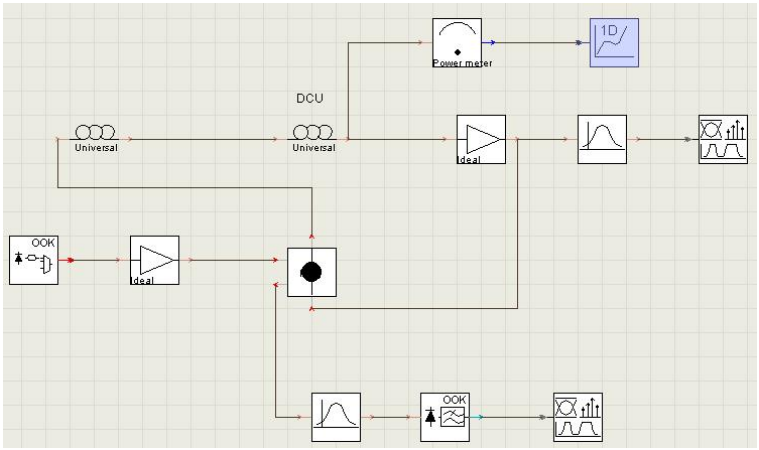

Figure 5.2: Network Simulation In VPI For In Band Monitoring.

5.2 Sample Network Analysis

We consider Deutsch Telekom network as a sample to determine the maximum length for the m-trail which can localize any single failure unambiguously. Parameters for the network are shown in Table 5.2. Besides, Figure 5.3 shows the topology for Deutsch Telekom network.

Table 5.2: Deutsch Telekom network parameters

Parameter	Value	
N	Number of Nodes	17.
L	Number Of Links (bidirectional)	26.
D	Network Diameter	7.
δ_{min}	Minimum Nodal Degree	2.
δ_{max}	Maximum Nodal Degree	6.
δ_{avg}	Average Nodal Degree	3.06.
α_{avg}	Physical Connectivity	0.19.
l_{min}	Shortest Link	36 km.
l_{max}	Longest Link	36 km.

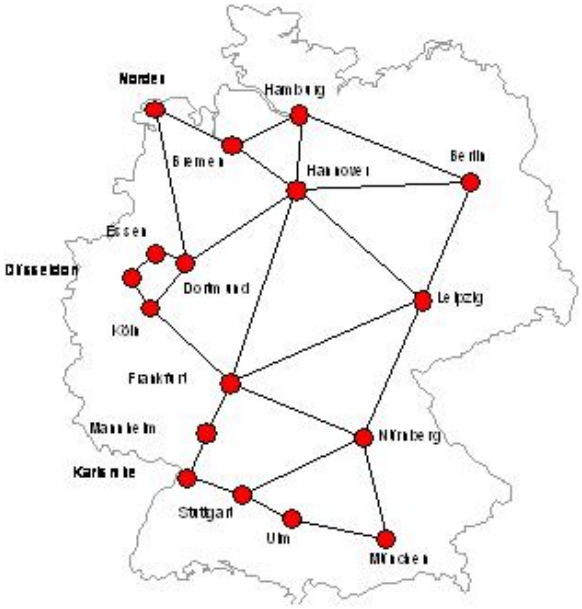

Figure 5.3: Topology Of Deutsch Telekom Network.

Based on the link's length, the maximum of length of each m-trail can be determined. Figure 5.2 shows the maximum m-trail for different number of m-trail.

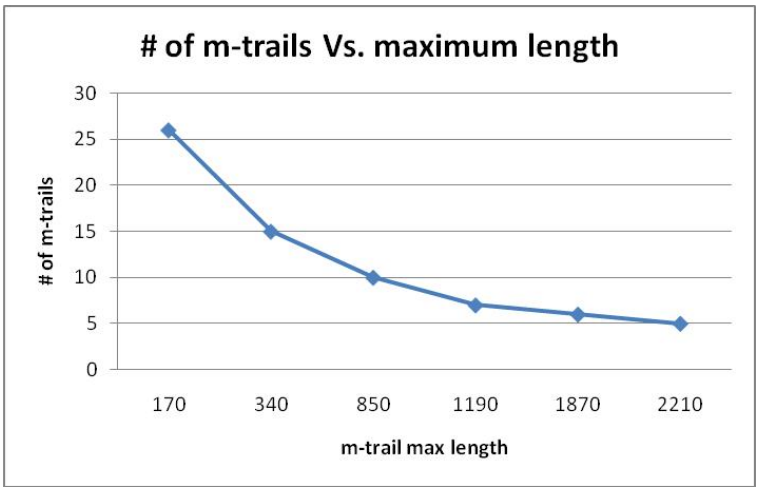

Figure 5.4: Number Of M-Trails vs. M-Trail Length In Deutsch Telekom Network.

The minimum number of m-trails is set to five as the theoretical lower limit for number of m-trails. Figure 5.2 shows that the maximum length for each m-trail should be 2210^{km} to localize each single failure unambiguously. This maximum length should be much bigger for large networks like USA reference network.

Chapter 6

Validation with Physical Layer Simulation

In the following, we consider two different scenarios: in-band monitoring and out of band monitoring.

6.1 In-Band Monitoring

In the case of in band monitoring, we investigate effect of different parameters which limit the m-trail length at the high bit rate simulation. We use VPI simulation to perform different scenarios for launching m-trail.

6.1.1 Effect Of Non-Linearity

Figure 6.1 shows the effect of non-linearity on length of the m-trail. The simulation is done at the 10 Gbps which is nominal in many practical systems.

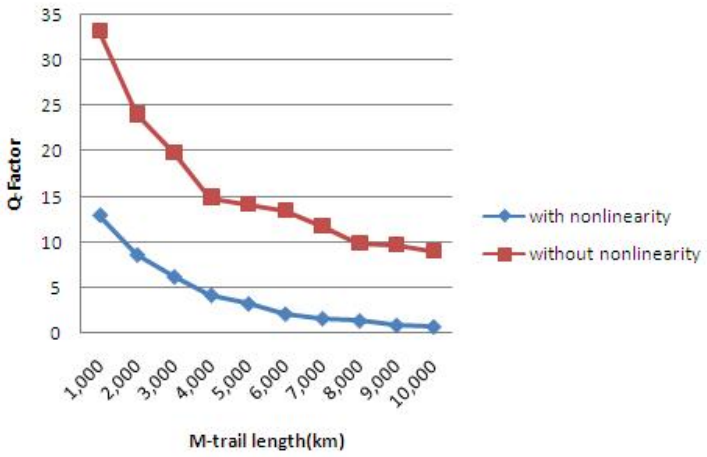

Figure 6.1: Q-Factor vs. Length Of M-Trail At 10 Gbps.

It can be seen that there is a huge difference between two cases. If we do not consider non-linearity, length of the m-trail can be increased over 10000^{km} without safe bound for BER and Q Factor but with considering non-linearity the maximum length cannot be exceeded over 4000^{km}. It shows that non-linearity is the most dominant parameter which limits length of the m-trail. However, by using special optical fibers, we can decrease the non-linear effects in fibers. Figure 6.2 shows the difference between two cases with different non-linear coefficient (core area of the fiber).

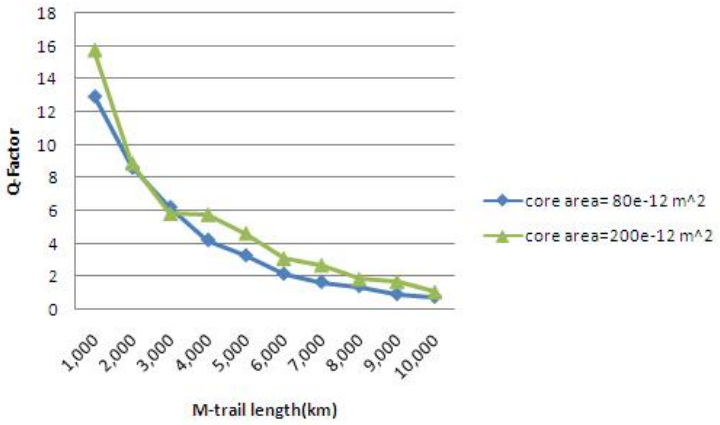

Figure 6.2: Q-Factor vs. Length Of M-Trail For Different Core Areas.

It can be seen that by decreasing non-linearity (increasing core area of the fiber) the maximum length can be increased up to 5000^{km}.

6.1.2 Effect Of Bit Rate

Figure 6.3 shows the effect of changing bit rate on length of the m-trail.

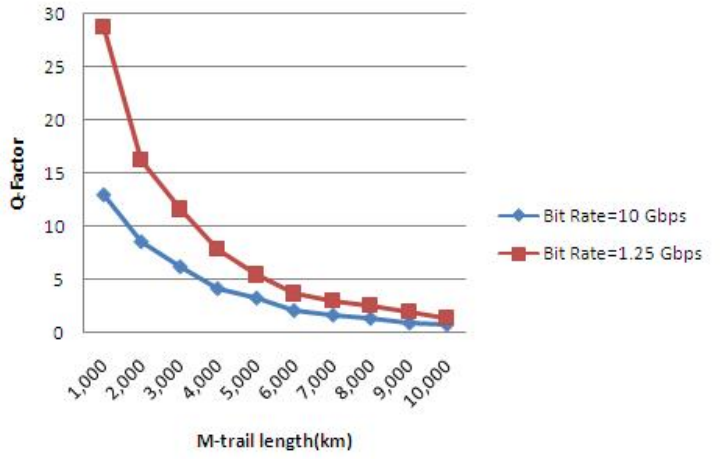

Figure 6.3: Q-Factor vs. Length Of M-Trail For Different Bit Rate.

As it can be seen in Figure 6.3, by decreasing the bit rate the maximum length of the m-trail can be increased up to 6000^{km}.

6.1.3 Effect Of Chromatic Dispersion

Figure 6.4 shows the effect of changing chromatic dispersion (CD) coefficient on length of the m-trail. The simulation is done for different CD scenarios. The simulation is done at the 10 Gbps which is nominal in many practical systems. Moreover, the non-linear effects are considered in the simulations.

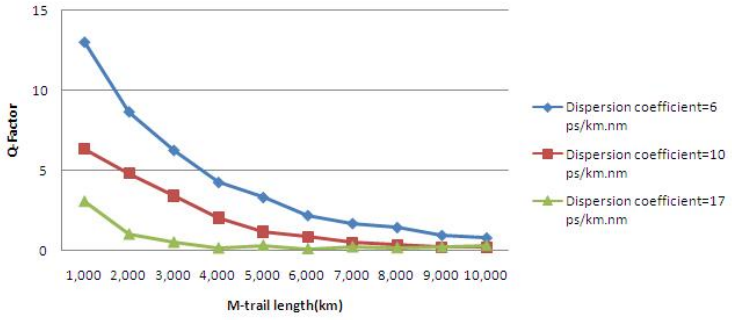

Figure 6.4: Q-Factor vs. Length Of M-Trail With Different CD Coefficient.

It can be determined when the dispersion coefficient is increased to 17 ps/km.nm (which is typical for many WDM networks), the m-trail maximum length decreases dramatically. It reaches to below 1000^{km} which is un-acceptable for m-trail length. It should be mention that by using non-zero dispersion shifted optical fibers (ITU-T G-655 standard), dispersion coefficient can be reduced significantly.
It can be seen that in the case of in-band monitoring, the maximum length for m-trail cannot reach 6000^{km} for bit rate of 10 Gbps which is not enough for large networks. So, I try to find better results in out of band monitoring where we are concern to establish the m-trail on the wavelength that carry the traffic.

6.2 Out Of Band Monitoring

In out of band monitoring scheme, we use two stage EDFA amplifiers to solve the problem of power loss in the network. In order to simulate out of band monitoring, we consider the Bit Rate to 1.5 Mbps it is used only for supervisory purpose.
We can reach the brilliant length of 18000^{km}. It should be mentioned that the dispersion coefficient is 17 ps/km.nm, which is typical for most WDM networks. Figure 6.5 shows the VPI simulation for out of band networks. Figure 6.6 shows the Q Factor versus m-trail for Figure 6.5.

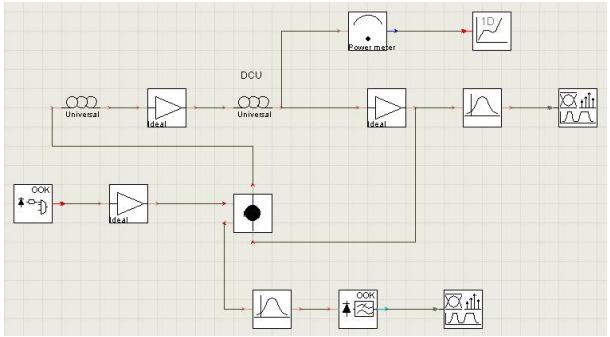

Figure 6.5: Network Simulation In VPI For Out Of Band Monitoring.

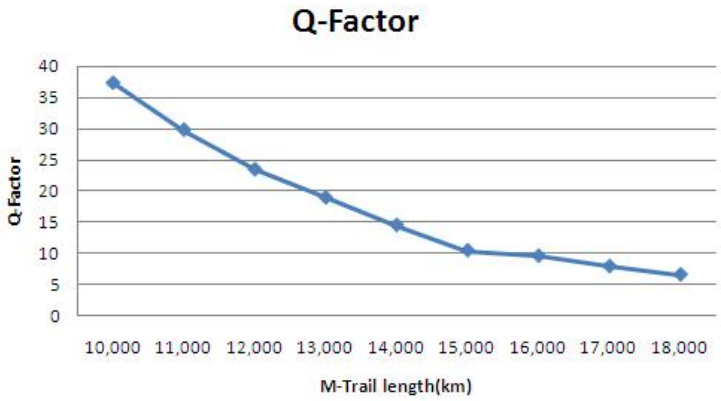

Figure 6.6: Q-Factor vs. Length For Out Of Band Monitoring Scheme.

In Figure 6.6, Q-factor for less than 10000^{km} is not considered because BER is zero for all those length. It can be determined that the length limit for m-trail increase significantly. Figure 6.7 shows the eye diagram for length of 18000^{km}.

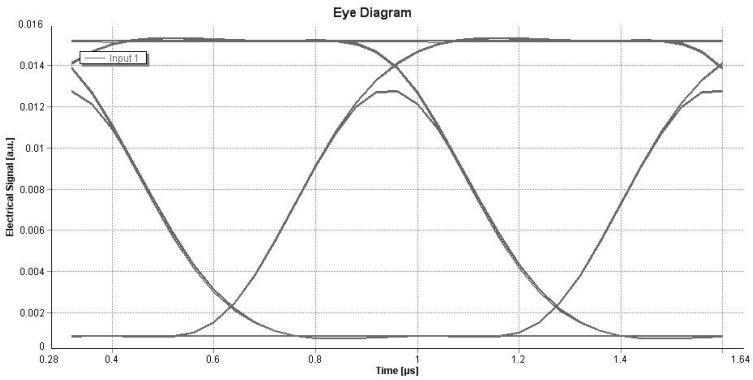

Figure 6.7: Eye Diagram For The Length Of 20000km.

Chapter 7

Conclusion

In this work, we have investigated the effect of several physical constraints which restrict the m-trail feasibility. It is supported by different simulations which are done in VPI transmission Maker Simulation Tool. Our simulations indicate that the length limit of m-trail can reach more than 18000^{km}. However, we use an error margin 5 for Q factor for possible stronger nonlinear impairments, additional noise in EDFA and uncompensated chromatic dispersion. So, with considering these factors, we reach the length limit of 13000^{km} for m-trail length which is sufficient for different backbone networks.
Besides, we examined several algorithms that form monitoring trails and compared their performance with a theoretical lower bound. We came to the conclusion that the ILP algorithm performs very well, yielding solutions close to the lower bound. We also examined the case of reducing the length of the longest m-trail in the network to half, and have observed that this multiplies the number of m-trails by an average of 1.7. The results can help significantly reduce the cost of monitoring without losing the fast and unambiguously failure localization.

Bibliography

[1] C. Assi, Y. Ye, A. Shami, S. Dixit, and M. Ali, "A hybrid distributed fault-management protocol for combating single-fiber failures in mesh based DWDM optical networks," in *IEEE GLOBECOM*, pp. 2676–2680, 2002.

[2] S. Stanic, S. Subramaniam, H. Choi, G. Sahin, and H. Choi, "On monitoring transparent optical networks," in *Int. Conference on Parallel Processing Workshops (ICPPW '02)*, pp. 217–223, 2002.

[3] H. Zeng, C. Huang, and A. Vukovic, "A novel fault detection and localization scheme for mesh all-optical networks based on monitoring-cycles," *Photonic Communication Networking*, pp. 277–286, 2006.

[4] S. Stanic, S. Subramaniam, G. Sahin, H. Choi, and H. A. Choi, "Active monitoring and alarm management for fault localization in transparent all-optical networks," *IEEE Transactions on Network and Service Management*, vol. 7, no. 2, pp. 118–131, 2010.

[5] J. Tapolcai, B. Wu, and P.-H. Ho, "On monitoring and failure localization in mesh all-optical networks," in *IEEE INFOCOM*, (Rio de Janero, Brasil), pp. 1008–1016, 2009.

[6] B. Wu, P.-H. Ho, and K. Yeung, "Monitoring trail:a new paradigm for fast link failure localization in WDM mesh networks," in *IEEE GLOBECOM*, 2008.

[7] H. Zeng and C. Huang, "Fault detection and path performance monitoring in meshed all-optical networks," in *IEEE GLOBECOM*, vol. 3, pp. 2014–2018, 2004.

[8] Zeng and Haung, "Spanning-tree based monitoringcycle construction for fault detection and localization in meshed alloptical networks," 2005.

[9] "VPI transmission Maker TM." http://www.vpiphotonics.com.

[10] B. Wu, P.-H. Ho, K. Yeung, J. Tapolcai, and H. Mouftah, "Optical Layer Monitoring Schemes for Fast Link Failure Localization in All-Optical Networks," *IEEE Communications Surveys & Tutorials*, vol. 13, pp. 114 –125, quarter 2011.

[11] A. Haddad, E. Doumith, and M. Gagnaire, "A meta-heuristic approach for monitoring trail assignment in WDM optical networks," in *Int. Workshop on Reliable Networks Design and Modeling (RNDM)*, pp. 601–607, IEEE, 2010.

[12] C. M. Machuca and M. Kiese, "Optimal placement of monitoring equipment in transparent optical networks," in *IEEE DRCN*, 2007.

[13] A. Haddad, E. A. Doumith, and M. Gagnaire, "A meta-heuristic approach for monitoring trail assingment in wdm optical networks," in *Iternational Congress on Ultra Modern Teleclommunications and Control Systems and Workshops (ICUMT)*, December 2010.

[14] B. Wu, P.-H. Ho, and K. L. Yeung, "Monitoring trail: On fast link failure localization in all-optical wdm mesh networks," *IEEE/OSA Journal of Lightwave Technology*, vol. 27, pp. 4175–4185, September 2009.

[15] A. Betker, C. Gerlach, R. Hülsermann, M. Jäger, M. Barry, S. Bodamer, J. Späth, C. Gauger, and M. Köhn, "Physical layer impairments in wdm core networks: a comparison between a north-american backbone and a pan-european backbone," in *5th ITG Workshop on Photonic Networks*, (Leipzig, Germany), May 2009.

[16] "Lion and cost 266 reference network." http://sndlib.zib.de.

[17] G. Katona, "On separating sets of a finite set," *Journal of Combinatorial Theory*, vol. 1, September 1966.

[18] I. Wegener, "On separating systems whose elements are sets of at most k elements," *Discrete Mathematics*, vol. 28, pp. 219 – 222, 1979.

[19] S. Azodolmolky, M. Klinkowski, E. Marin, D. Careglio, J. S. Pareto, and I. Tomkos, "A survey on physical layer impairments aware routing and wavelength assignment algorithms in optical networks," *Computer Networks*, vol. 53, pp. 926–944, 2009.

[20] S. Al Zahr, M. Gagnaire, N. Puech, and M. Koubaa, "Physical Layer Impairments in WDM Core Networks: a Comparison between a North-American Backbone and a Pan-European Backbone," in *Broadband Networks*, vol. 2, pp. 1258 – 1263, 2005.

[21] M. Farahmand, D. Awduche, S. Tibuleac, and D. Atlas, "Characterization and representation of impairments for routing and path control in all-optical networks," in *National Fiber Optic Engineers*, National Fiber Optic Engineers Conference (NFOEC-2002), 2002.

[22] D. Emmanuel, *Erbium-Doped Fiber Amplifiers*. John Wiley & Sons, 1994.

[23] G. P. Agrawal, *Fiber-Optic Communication Systems*. John Wiley & Sons, 2002.